Pramana – J. Phys. (2017) 88: 32
DOI 10.1007/s12043-016-1341-4

The effects of Mg incorporation and annealing temperature on the physicochemical properties and antibacterial activity against *Listeria monocytogenes* of ZnO nanoparticles

NIMA SHADAN[1], ALI ABDOLAHZADEH ZIABARI[2,*], RAFIEH MERAAT[3] and KAMYAR MAZLOUM JALALI[1]

[1]Department of Microbiology, Faculty of Science, Science and Research Branch of Guilan, Islamic Azad University, Rasht, Iran
[2]Nano Research Lab, Lahijan Branch, Islamic Azad University, P.O. Box 1616, Lahijan, Iran
[3]Department of Microbiology, Faculty of Science, Lahijan Branch, Islamic Azad University, Lahijan, Iran
*Corresponding author. E-mail: ali.abd.ziabari@gmail.com

MS received 10 November 2015; revised 25 May 2016; accepted 29 July 2016; published online 9 January 2017

Abstract. In this paper, Mg-doped ZnO nanoparticles were synthesized by the facile sol–gel method. The crystalline structure, characteristic absorption bands and morphology of the obtained Mg-doped ZnO nanoparticles were studied by XRD, FTIR and TEM. The thermal degradation behaviour of the samples was investigated by differential scanning calorimetry (DSC) and thermogravimetry (TG). The effect of Mg concentrations and annealing temperatures on the antibacterial properties of the obtained nanoparticles was investigated in detail. The results indicated that doping Mg ions into ZnO lattice could enhance its antibacterial activity. Antibacterial assay demonstrated that Mg-doped ZnO with 7% Mg content annealed at 400°C had the strongest antibacterial activity against *Listeria monocytogenes* (98.7%). This study indicated that the inhibition rate of ZnO nanoparticles increased with the formation of granular structure and the decrease of ZnO size due to the doping of Mg ions into the ZnO lattice.

Keywords. ZnO:Mg; nanoparticles; physicochemical properties; *Listeria monocytogenes*.

PACS Nos 81; 78.20.–e; 78

1. Introduction

Bacterial contamination is a serious concern in healthcare and food industry, and so developing antibacterial agents has caught increasing attention in recent years. It has been found that the toxicity of nanoparticles is more severe than that of larger particles of the same materials [1]. Therefore, developing nanoparticles with antimicrobial properties are of considerable interest. Recent studies demonstrate that ZnO nanostructures can be used effectively against both gram-positive and gram-negative bacteria [2,3]. As a wide band-gap semiconductor, zinc oxide (ZnO) has been considered as an ideal antibacterial agent because its biocompatibility, stability and reusability are better than organic antibacterial agents [4]. It has been recognized that, beside morphology, shape and size of ZnO nanoparticles, adding dopants into ZnO host matrix can tune its various properties and increase the related antibacterial activity [5,6]. Magnesium oxide (MgO) has a band gap of 7.8 eV and has a cubic crystal structure. When Mg is doped into ZnO, more surface defects are produced, hindering the recombination of photoinduced electron–hole pairs. This helps to improve the photocatalytic activity. Also, doping of Mg in ZnO significantly induces the defects in the band structure of ZnO and tailors its band gap. Therefore, it is expected that Mg doping can strongly affect the antibacterial activity of ZnO nanoparticles. Iqbal *et al* [7] have reported strong antibacterial activity of coprecipitated Mg-doped ZnO nanostructures against *S. aureus*. To the best of our knowledge, reports on the effect of Mg-doped ZnO nanostructures against *Listeria monocytogenes* are rare.

Listeria monocytogenes bacterium is a food-borne pathogen that causes Listeriosis and can cause meningitis and sepsis in newborns and adults with weakened immune systems, encephalitis, abortions in both animals and the humans.

In this study, Mg-doped ZnO nanopowderes with varying Mg doping levels (i.e. 0, 1, 3, 5 and 7 at%) were synthesized by cost-effective, low temperature and facile sol–gel method. Two annealing temperatures were also considered. Some physical properties along with the antibacterial activity of the synthesized nanostructures were studied.

2. Experimental section

2.1 *Fabrication of Mg-doped ZnO nanoparticles*

For the synthesis of undoped and Mg-doped ZnO nanostructures, analytical-grade zinc acetate dihydrate ($Zn(CH_3COO)_2{\cdot}2H_2O$) and magnesium acetate ($Mg(C_2H_3O_2)_2$), were used as the precursor and ethanol and diethanolamine as the solvent and the stabilizer.

Three separate solutions of zinc acetate dihydrate, magnesium acetate and diethanolamine were prepared and stirred separately for 1 h at room temperature. Then zinc acetate and diethanolamine solutions were mixed together and stirred for 0.5 h at room temperature.

Different amounts of magnesium acetate solution was added to the above-mentioned mixture to obtain various (0, 1, 3, 5 and 7 at%) Mg doping levels. For the decomposition of the organic matter, samples were heated in an oven at 110°C for 3 h. Finally, to prepare ZnO:Mg nanopowders, the samples were annealed in air at two different annealing temperatures of 400 and 500°C.

2.2 *Characterization*

The structure of the samples was studied by X-ray diffraction (XRD) method using a XRD6000, Shimadzu system with CuK_α radiation (0.15406 nm). The diameter and size distribution of various NPs were measured by a transmission electron microscope (TEM) (CM120, Philips, Netherlands). Energy-dispersive X-ray (EDX) spectroscopy was done using a Philips X130 spectrometer. Fourier transform infrared spectroscopy (FTIR) absorption was measured for KBr supported samples over a frequency range of 4000–400 cm^{-1} and at a resolution of 4 cm^{-1}, using a model SHIMADZU, FTIR-8400S. To characterize the decomposition and thermal stability of the prepared samples, differential scanning calorimetry (DSC) and thermogravimetric analysis (TGA) were carried out (TA-Instants 951, manufactured by Dupont) in temperatures ranging from room temperature to 600°C and the heating rate was 10°C/min.

2.3 *Determination of antibacterial activity*

L. Monocytogenes cultures were kindly provided by Iranian Research Organization for Science and Technology (IROST). The bacterial strains were grown in brain heart infusion (BHI) broth culture medium (Merck) and incubated at 37°C for 18 h, followed by culturing in BHI agar medium (Merck) to give pure colonies. For the antibacterial measurement, bacterial cultures were routinely incubated at 37°C in Mueller Hinton broth (MH broth). The cells were harvested from log phase culture by centrifugation and subsequently washed and suspended into sterile PBS to achieve turbidity equivalent to 0.5 MacFarland. To prepare the colloidal suspension of the synthesized nanostructures, 0.06 mg of ZnO:Mg nanoparticles were added to 6 ml of MH broth and incubated at 37°C. Nanostructures-free culture grown under the same conditions was used as a control. Growth curves of these microbial strains were monitored by UV–visible spectrophotometer at a wavelength of 600 nm.

3. Results and discussion

3.1 *Physicochemical properties*

XRD results of the obtained pure and Mg-doped ZnO are shown in figure 1a. The diffraction peaks of the synthesized ZnO samples were quite similar to those of the crystalline wurtzite ZnO structure (JCPDS standard card 36-1451). No other characteristic peaks of the impurities appeared. Normally, incorporation of the dopant can influence the change of lattice strain and defects. However, in the present study, it was observed that the location of the peaks and the shape did not change with Mg doping. This is due to the similarity of ionic radius of Mg^{2+} (0.57 Å) and Zn^{2+} (0.60 Å). Therefore, replacement of Zn by Mg should not cause a significant change in lattice constants. However, with annealing temperature the peak intensities increased and the crystallization of ZnO enhanced. The average crystallite sizes of all the prepared samples are calculated using the Scherrer formula [8]. The average

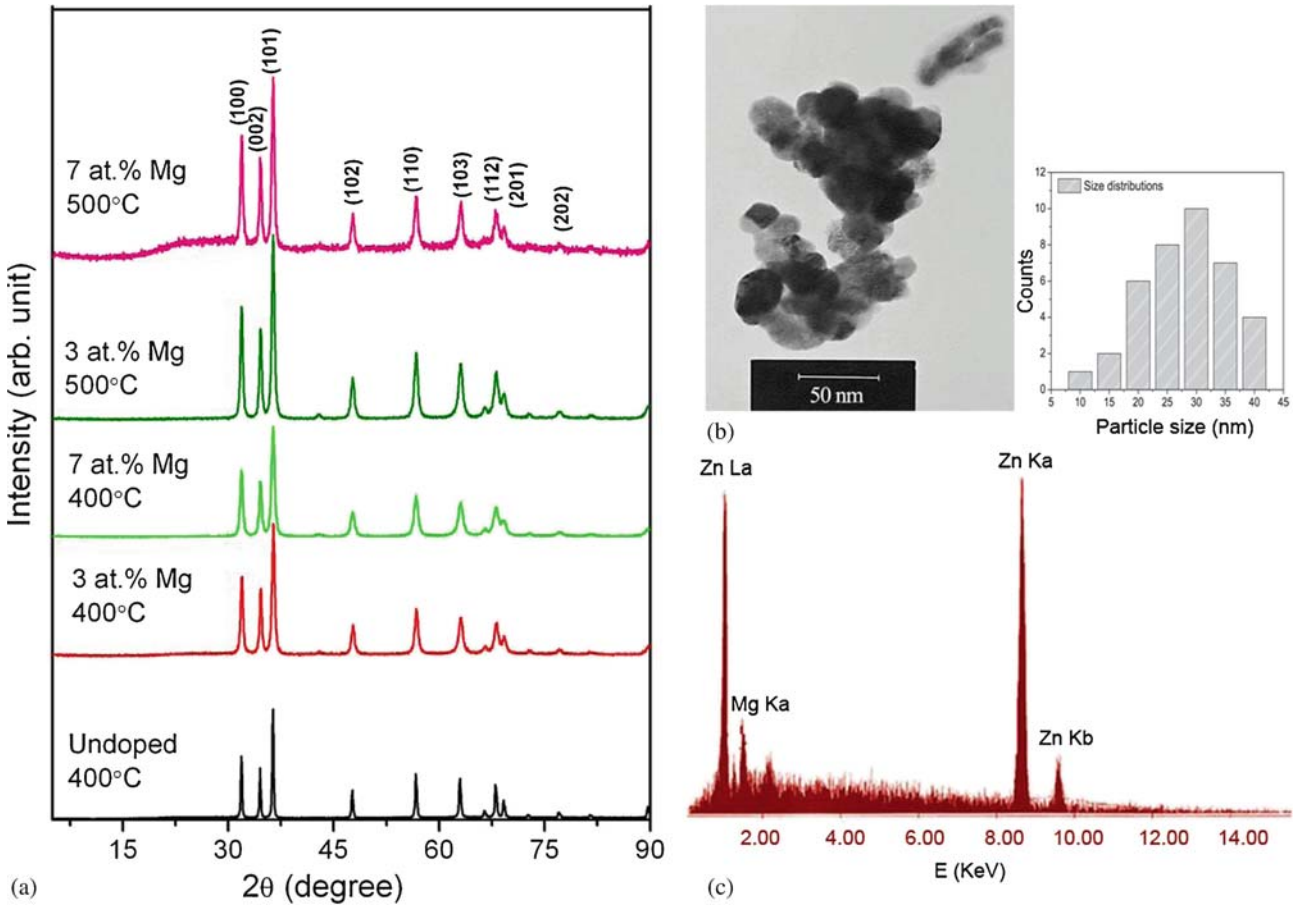

Figure 1. (**a**) XRD patterns of Mg-doped ZnO samples annealed at 400 and 500°C, (**b**) TEM image along with histogram indicating the size distribution of nanoparticles and (**c**) EDX spectrum for 7 at% Mg-doped ZnO nanopowder annealed at 400°C.

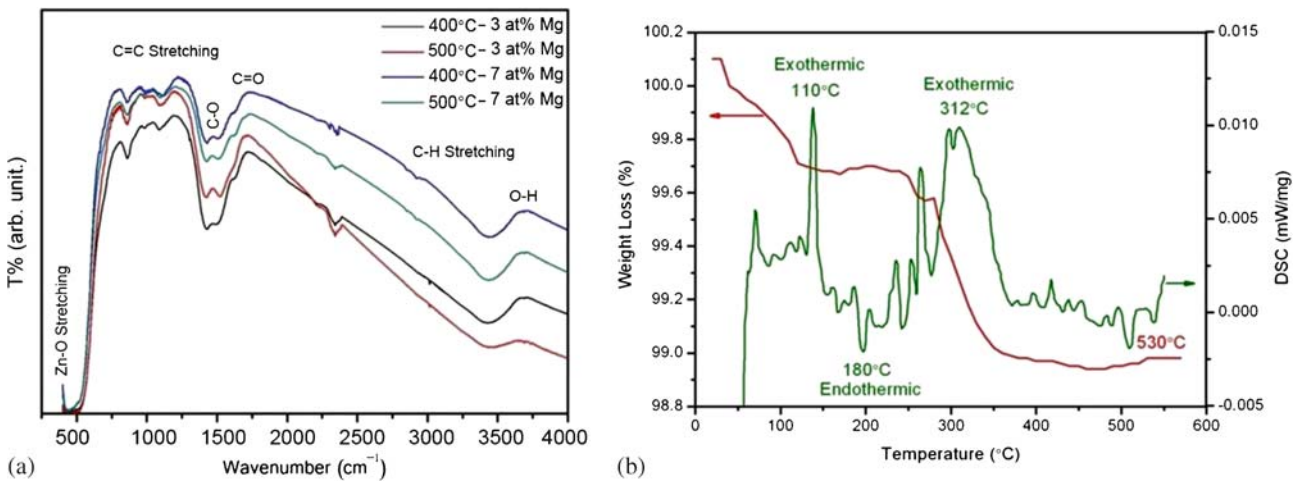

Figure 2. (**a**) FTIR spectra of Mg-doped ZnO nanoparticles annealed at 400 and 500°C and (**b**) DSC–TGA curves of 7 at% Mg-doped ZnO nanoparticles annealed at 400°C.

crystallite sizes are found to decrease/increase with increase in Mg content/annealing temperature, i.e. from 25.23 ± 0.55 nm/30.56 ± 0.47 nm for undoped ZnO to 24.29 ± 0.60 nm/27.44 ± 0.35 nm for 7% Mg-doped ZnO annealed at 400°C/500°C. The decrement of crystallite size with Mg doping can be linked to smaller ionic radii of Mg^{2+} compared to Zn^{2+}. The TEM micrograph along with size distribution

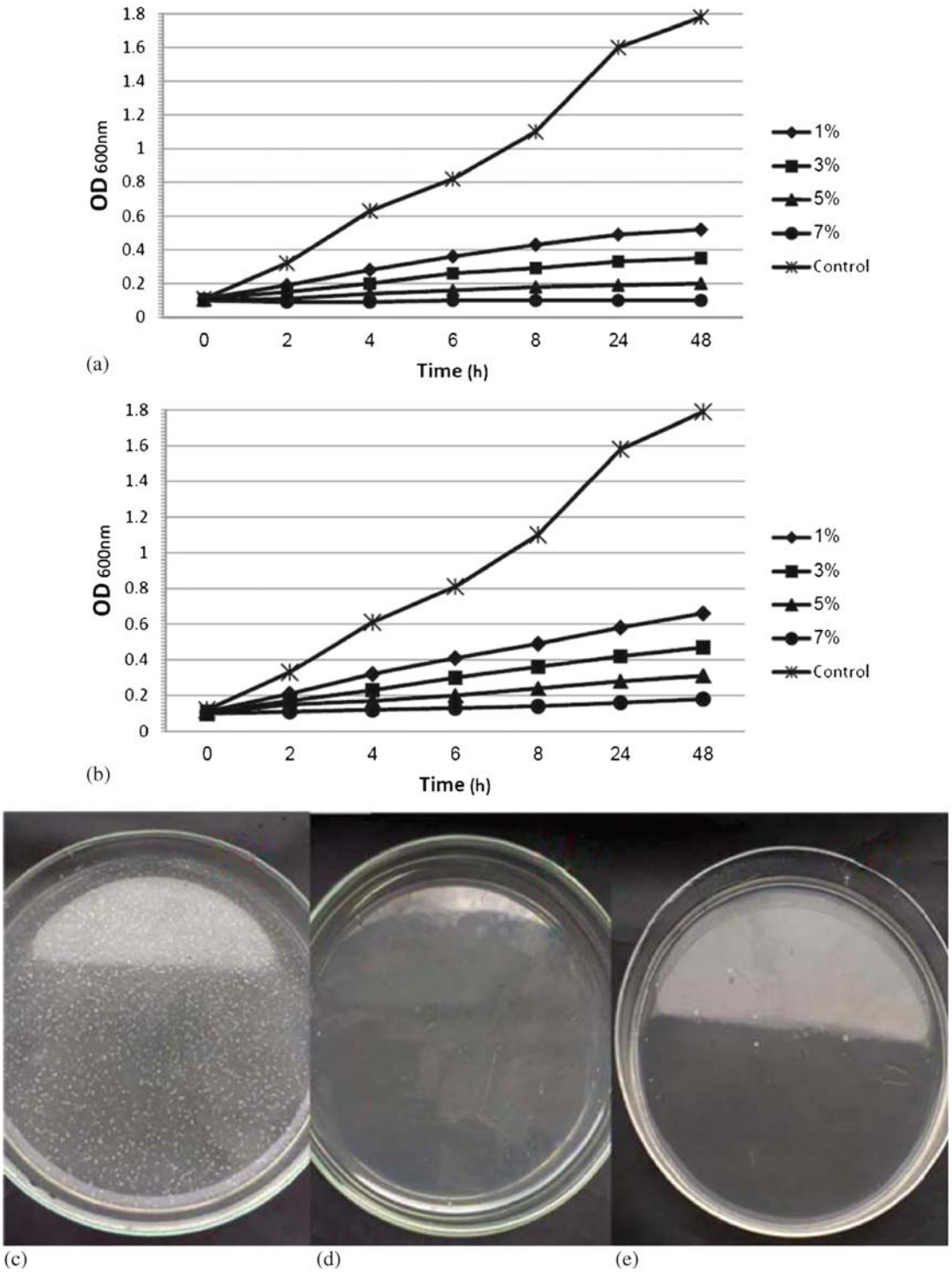

Figure 3. Growth curves for *L. monocytogenes* bacterial strain in the presence of Mg-doped ZnO nanostructures annealed at (**a**) 400°C and (**b**) 500°C. (**c**) Control of *L. monocytogenes* treated by 7 at% Mg-doped ZnO annealed at (**d**) 400°C and (**e**) 500°C. The samples were treated with 300 μl of the prepared colloidal suspension of the nanostructures.

histogram of the 7 at% Mg-doped ZnO nanoparticles annealed at 400°C are presented in figure 1b. As shown in the figure, most of the particles are quasispherical and the related size is mainly distributed between 25 and 30 nm. To calculate the particle size from XRD, all peaks were used and an average was taken. However, TEM scans the population of the particles directly. Therefore, there will be some difference between the

particle sizes obtained from XRD and TEM. The related EDX analysis results showed that the surface composition of Zn:O:Mg was 58.12:37.19:4.69, implying that the doping concentration of Mg was lower than that of nominal value (figure 1c).

FTIR analysis has been done to study the surface chemistry and modes of vibrations of chemical bonds present in all the prepared samples (figure 2a). The 3270 cm^{-1} band corresponds to the hydroxyl band, i.e. O–H mode, 1630 cm^{-1} band corresponds to the symmetric C=O stretching mode, ∼1220 cm^{-1} and ∼1350 cm^{-1} bands correspond to the asymmetric C–O stretching mode. The absorption band around 440 cm^{-1} can be assigned to the typical wurtzite phase of ZnO [9].

TGA transition shows a loss of 1.062% (0.07673 mg) up to 350°C (figure 2b). No considerable weight loss is observed after this up to 600°C. It simply indicates that when $Zn(OH)_2$ is heated, it converts into ZnO and that is stable above 350°C. So, for the formation of zinc oxide, temperature above 350°C is required. This is one reason for choosing 400 and 500°C as annealing temperatures in the present study. One large endothermic peak and two exothermic peaks were found in the DSC curve of ZnO sol (figure 2b).

Endothermic peaks such as peak at 180°C may be attributed to water evaporation and organic materials. The major observation is the exothermic peaks, particularly the peak located in 312°C, which may be due to crystallization of zinc oxide.

3.2 *Antibacterial activity*

The antibacterial assay of the prepared nanostructures towards *L. monocytogenes* was performed using optical density (OD) method or culture turbidity as qualitative measure of cell growth. Growth curves were recorded in the presence of the colloidal suspension of synthesized nanostructures. Figures 3a and 3b show the growth curves for *L. monocytogenes* after its interaction with Mg-doped ZnO nanostructures annealed at 400 and 500°C, respectively. It can be seen from the figure that in the case of the control sample, bacterial strains show exponential growth. But in the presence of Mg-doped ZnO nanostructures, the growth decreased drastically. Highest Mg-doped sample, i.e. 7 at%, annealed at lower temperature, i.e. 400°C, showed almost no growth during 48 h. As can be seen from the figure, higher/lower Mg content/annealing temperature causes more efficient antibacterial activity against *L. monocytogenes*.

Table 1. Inhibition rate of *L. monocytogenes* treated with Mg-doped ZnO nanopowders.

$T_{\text{Annealing}}$	1 at% Mg	3 at% Mg	5 at% Mg	7 at% Mg
400°C	70.5%	82%	91%	98.7%
500°C	64.1%	75.6%	88.4%	96.1%

L. monocytogenes was used for colony forming unit (CFU) measurements on the solid medium plate. Samples treated with 300 μl of the prepared suspension of ZnO:Mg nanoparticles were spread on nutrient agar plates. After incubation at 37°C for 48 h, the numbers of CFU were counted (figures 3c–3e).

The inhibition rates of the samples against *L. monocytogenes* were determined by counting the number of CFU according to the formula (inhibition rate $= (N_0 - N_t)/N_0 \times 100\%$, where N_0 is the number of *L. monocytogenes* without the treatment of ZnO:Mg and N_t is the number of *L. monocytogenes* treated by ZnO:Mg for 48 h). The specific values are shown in table 1. It can be seen that 7 at% Mg-doped ZnO has the strongest antibacterial activity among the tested samples. The inhibition rates of 7 at% Mg-doped ZnO samples annealed at 400°C and 500°C were 98.7% and 96.1%, respectively. The increment of antibacterial activity of ZnO with Mg doping may be due to the variation in grain size, morphology and soluble Zn^{2+} ions. All these factors are reported to have strong influence on the antibacterial activity of ZnO [10]. The antibacterial activity of nanostructures is mainly due to their small size which is smaller than the size of the bacterium. Due to smaller sizes they can easily adhere to the cell wall of the bacterium, causing its destruction leading to the death of the bacterium [11].

4. Conclusion

In summary, Mg-doped ZnO nanoparticles were prepared by a facile sol–gel method. The effect of annealing temperature was also studied. The pertinent XRD, EDS, TEM, FTIR, TGA–DSC and antibacterial assay results were studied and linked together. All the prepared samples showed great antibacterial activity. Particularly, 7 at% Mg-doped ZnO nanoparticles annealed at 400°C showed the strongest inhibition rate against *L. monocytogenes* (98.7%).

References

[1] K H Tam, A B Djurisic, C M N Chan, Y Y Xi, C W Tse, Y H Leung, W K Chan, F C C Leung and D W T Au, *Thin Solid Films* **516**, 6167 (2008)

[2] R R Krishna, T K Ranjit and C M Adhar, *Langmuir* **27**, 4020 (2011)
[3] J Nicole, R Binata, T R Koodali and C M Adhar, *FEMS Microbiol. Lett.* **279**, 71 (2008)
[4] W W He, H K Kim, W G Wamer, D Melka, J H Callahan and J J J Yin, *Am. Chem. Soc.* **136**, 750 (2014)
[5] K S Ranjan, K Ganguly, T Mishra, M Mishra, R S Ningthoujam, S K Roy and L C Pathak, *J. Colloid Interface Sci.* **366**, 8 (2012)
[6] S S Clament, V Judith and K John, *J. Colloid Interface Sci.* **407**, 215 (2013)
[7] J Iqbal, T Jana, M Ismail, N Ahmad, A Arif, M Khan, M Adil, Sami-ul-Haq and A Arshad, *Ceram. Int.* **40**, 7487 (2014)
[8] B D Cullity and S R Stock, *Elementary of X-ray diffraction*, 3rd edn (Prentice-Hall, Englewood Cliffs, New Jersey, 2001)
[9] Y J Kwon, K H Kim and C S Lim, *J. Ceram. Proc. Res.* **3**, 146 (2002)
[10] T Nasrin, M A Seyedeh and D Monir, *J. Photochem. Photobiol. B*: *Biol.* **120**, 66 (2013)
[11] M Y Jehad and N D Enas, *J. Health Sci.* **2**, 38 (2012)